

# Chaotic background of large-scale climate oscillations

A. Bershadskii

*ICAR - P.O. Box 31155, Jerusalem 91000, Israel*

---

## Abstract

It is shown that the periodic alteration of night and day provides a chaotic dissipation mechanism for the North Atlantic (NAO) and Southern (SOI) climate oscillations. The wavelet regression detrended daily NAO index for last 60 years and daily SOI for last 20 years as well as an analytical continuation in the complex time domain were used for this purpose.

*Keywords:* Chaos, climate oscillations, complex time, atmosphere

---

”And in the alteration of night and day,  
and the food We send down from the sky,  
and revives therewith the earth after its  
death, and in the turning about of winds  
are signs for people of understanding”.

QURAN (45:4-5).

## 1. Introduction

It is now well known that climate is a nonlinear system. The nonlinear systems can exhibit a chaotic behavior. Both stochastic and deterministic processes can result in the broad-band part of the spectrum, but the decay in the spectral power is different for the two cases. The *exponential* decay indicates that the broad-band spectrum for these data arises from a deterministic rather than a stochastic process (cf. Figs. 1-4). For a wide class of deterministic systems a broad-band spectrum with exponential decay is a generic feature of their chaotic solutions (Ohtomo et al. 1995; Farmer 1982; Sigeti 1995; Frisch and Morf 1981). Also response of the chaotic systems to the periodic forcing does not always have the result that one might expect. Unlike linear systems, where periodic forcing leads to a periodic (peak-like) response, the chaotic response to periodic forcing can result in modification of

the rate of the exponential decay of the broad-band power spectrum. Thus, the chaotic response to periodic forcing can utilize the generic dissipation mechanism for the chaotic dissipative systems, especially in the case when the system's fundamental (internal) frequency is considerably lower than the frequency of the periodic forcing under consideration.

The climate, where the chaotic behavior was discovered for the first time, is still one of the most challenging areas for the theory of chaos. The weather (time scales up to several weeks) chaotic behavior usually can be directly related to chaotic convection, while appearance of the chaotic properties for more long-term climate events is a non-trivial and challenging phenomenon.

The solar day is a period of time during which the earth makes one revolution on its axis relative to the sun. During a part of the day the sun's direct rays are blocked (locally) by the earth. Therefore, the periodic *daily* variability of solar impact plays crucial role in high frequency climate behavior. It will be shown in present paper that just unusual properties of chaotic response to the daily periodicity of solar forcing provide an effective mechanism for high frequency dissipation of the large-scale climate oscillations, presumably generated by the instabilities related to large scale topography.

## 2. Large-scale climate oscillations

One of the most significant and recurrent patterns of atmospheric variability over the middle and high latitudes of the Northern Hemisphere is known as NAO - North Atlantic Oscillation. Climate variability from the subtropical Atlantic to the Arctic and from Siberia to the eastern boards of the North America is strongly related to the NAO (see, for a comprehensive review Hurrell et al. (2003)). In site NAO (2010a) a projection of the daily 500mb height anomalies over the Northern Hemisphere onto the loading pattern (see also NAO, 2010b) of the NAO was used in order to construct the daily NAO for last 60 years. Due to the natural climatic trends the daily NAO index time series is not a statistically stationary data set. In order to solve this problem a wavelet regression detrending method (Ogden, 1997) was used in present investigation for the daily NAO time series. We used a symmlet regression of the data. Most of the regression methods are linear in responses. At the nonlinear nonparametric wavelet regression one chooses a relatively small number of wavelet coefficients to represent the underlying regression function. A threshold method is used to keep or kill the wavelet coefficients. In this case, in particular, the Universal (VisuShrink)

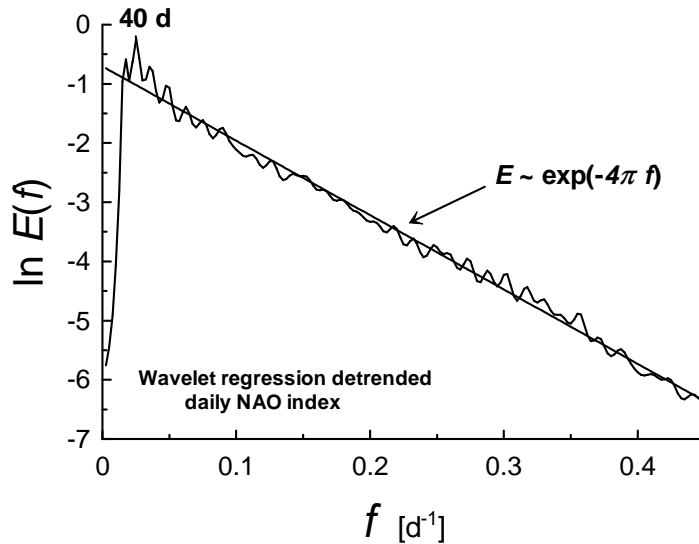


Figure 1: Spectrum of the wavelet regression detrended NAO data series (the NAO index data were taken from the site NAO, 2010a). In the semi-logarithmic scales used in the figure the straight line indicates the exponential decay Eq. (1).

thresholding rule with a soft thresholding function was used. At the wavelet regression the demands to smoothness of the function being estimated are relaxed considerably in comparison to the traditional methods. Figure 1 shows a spectrum of the wavelet regression detrended data (NAO, 2010a) calculated using the maximum entropy method. This method provides an optimal spectral resolution even for small data sets. The spectrum exhibits a broad-band behavior with exponential decay:

$$E(f) \sim e^{-4\pi f} \quad (1)$$

A semi-logarithmic plot was used in Fig. 1 in order to show the exponential decay (at this plot the exponential decay corresponds to a straight line, for an explanation see below).

Another example of the large-scale climate oscillations with the chaotic dissipation mechanism can be recognized in Tropical Atmosphere, where one of the most significant and recurrent patterns of atmospheric variability between the western and eastern tropical Pacific is known as Southern Oscillation. The Southern Oscillation is related to the variability of the Walker circulation system: a circulation pattern characterized by sinking air above the eastern Pacific and rising air above the western Pacific. The Southern Oscillation is often considered as the atmospheric component of *El Niño*

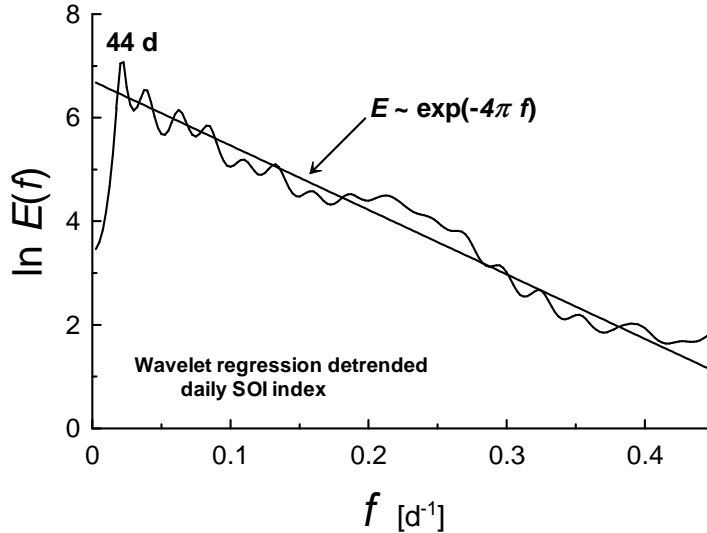


Figure 2: Spectrum of the wavelet regression detrended SOI data series (the SOI data were taken from the site SOI, 2010). In the semi-logarithmic scales used in the figure the straight line indicates the exponential decay Eq. (1).

phenomenon. The daily Southern Oscillation Index (SOI) has been calculated based on the differences in air pressure anomaly between Tahiti and Darwin, Australia (Troup, 1965) for last 20 years (SOI, 2010). Figure 2 shows a spectrum of the wavelet regression detrended data calculated using the maximum entropy method. A semi-logarithmic plot was used in Fig. 2 in order to show the exponential decay Eq. (1) (cf Fig.1).

### 3. Chaos and exponential spectrum

For a wide class of deterministic systems a broad-band spectrum with exponential decay is a generic feature of their chaotic solutions (Ohtomo et al. 1995; Farmer 1982; Sigeti 1995; Frisch and Morf 1981). Let us consider a relevant example. The Lorenz equations are given by:

$$\frac{dx}{dt} = \sigma(y - x), \quad \frac{dy}{dt} = rx - y - xz, \quad \frac{dz}{dt} = xy - bz \quad (2)$$

The standard values producing a chaotic attractor are:  $\sigma = 10.0$ ,  $r = 28.0$ ,  $b = 8/3$ . Figure 3 shows a power spectrum for  $z$ -component of the Lorenz chaotic attractor generated by Eq. (2) (the spectrum was again calculated using the maximum entropy method). A semi-logarithmic plot was

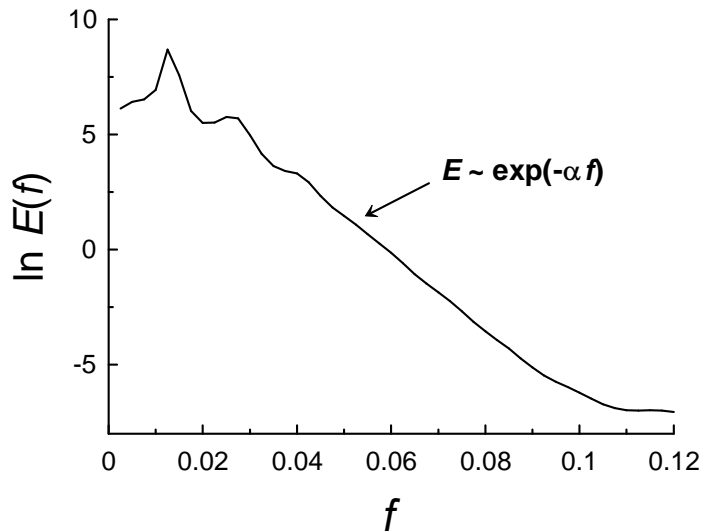


Figure 3: As in Fig.1 but for  $z$ -component of the Lorenz chaotic attractor Eq. (2). In the semi-logarithmic scales used in the figure the straight line indicates the exponential decay.

used again in Fig. 2 in order to show exponential decay (at this plot the exponential decay corresponds to a straight line).

Another relevant example is a modulated Duffing oscillator. The driven Duffing oscillator has become a classic model for analysis of nonlinear phenomena and can exhibit both deterministic and chaotic behavior: Ott, 2002; Permann and Hamilton, 1992). It is well known that for strong nonlinearity a driven Duffing oscillator can exhibit chaotic properties and, in particular, exponentially decaying broad-band spectrum (see, for instance, Ohtomo et al. (1995)). In the case of a weak nonlinearity, however, one needs in an additional slow modulation of the driving force in order to obtain a chaotic behavior. In this case a separation between fast and slow motion is possible and in certain range of parameters the slow component exhibits chaotic properties with an exponentially decaying broad-band spectrum (see, for instance, Miles (1984)). The driven Duffing oscillator is described by the equation

$$\ddot{x} + \omega_0^2 x(1 + \eta x^2) + 2\delta\omega_0 \dot{x} = A(t)\cos(\omega_c t) \quad (3)$$

where  $\dot{x}$  denotes the temporal derivative of  $x$ ,  $\delta$  is a damping parameter,  $\eta$  is a nonlinearity parameter,  $\omega_0$  is the natural frequency for free oscillations,  $\omega_c$  is the carrier frequency. The amplitude  $A(t)$  can be slow modulated. Namely,  $A(t) = \varepsilon\omega_0^2\cos(\omega_m t + \theta_0)$ , where  $\omega_m$  is a modulation frequency,  $\theta_0$

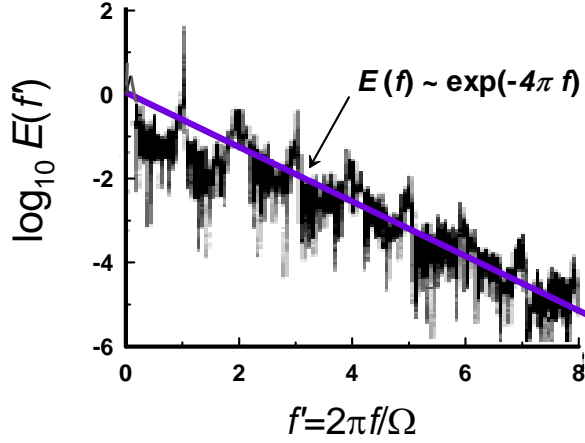


Figure 4: As in Fig.3 but for slow component of the modulated Duffing oscillator. In the semi-logarithmic scales used in the figure the straight line indicates the exponential decay. The data were taken from Miles (1984).

is a phase constant,  $\varepsilon$  is a small constant amplitude. Except of a resonant domain:  $(\omega_c^2 - \omega_0^2)/\omega_0^2$  and  $\omega_m/\omega_0 = O(\varepsilon^{2/3})$  the nonlinearity is unimportant in the limit  $\varepsilon \rightarrow 0$ . Following to Miles (1984) one can introduce a slow time  $\tau = \frac{1}{2}\sigma\omega_c t$  and pose the solution of Eq. (3) in the form (Van der Pol transformation):

$$x(t) = \frac{\varepsilon}{\sigma} [u_1(\tau)\cos(\omega_c t) + u_2(\tau)\sin(\omega_c t)] \quad (4)$$

where  $u_1(\tau)$  and  $u_2(\tau)$  are slowly varying amplitudes,  $\sigma \sim O(\varepsilon^{2/3})$  is an arbitrary dimensionless positive constant.

Then the equations for the slow components are

$$\frac{du_1}{d\tau} = U_1(u_1, u_2), \quad \frac{du_2}{d\tau} = U_2(u_1, u_2) + \cos\theta \quad (5)$$

where  $\theta = \Omega\tau + \theta_0$ ,  $\Omega = 2\omega_m/\sigma\omega_c$ , and  $U_1(u_1, u_2)$  and  $U_2(u_1, u_2)$  are certain linear functions on  $u_1$  and  $u_2$  (see for more details Miles (1984)). Numerical analysis of the equations (5) performed by Miles (1984) showed that for certain values of the parameters the slow component of the oscillations exhibits chaotic properties. In particular, the broad-band spectra with exponential decay were observed by Miles (1984) for these values of parameters. Figure 4 shows an example of such spectrum ( $\Omega = 0.75$ , the data were taken from Miles (1984)). The spectra were calculated by Miles (1984) using a fast-Fourier-transform with frequency  $f \longleftrightarrow \tau$ . One can see a clear peak corresponding to the fundamental frequency  $f_{fun} = \Omega/2\pi$ . We have drawn the straight line in Fig. 4 in order to indicate the exponential decay: Eqs.

(1). The same exponential decay - Eq. (1), can be observed for all 'chaotic' values of the parameter  $\Omega$ , i.e. it has an universal nature.

Nature of the exponential decay of the power spectra of the chaotic systems is still an unsolved mathematical problem. A progress in solution of this problem has been achieved by the use of the analytical continuation of the equations in the complex domain (see, for instance, Frisch and Morf (1981)). In this approach the exponential decay of chaotic spectrum is related to a singularity in the plane of complex time, which lies nearest to the real axis. Distance between this singularity and the real axis determines the rate of the exponential decay. For many interesting cases chaotic solutions are analytic in a finite strip around the real time axis. This takes place, for instance for attractors bounded in the real domain (the Lorenz attractor, for instance). In this case the radius of convergence of the Taylor series is also bounded (uniformly) at any real time. Let us consider, for simplicity, solution  $u(\tau)$  with simple poles only, and to define the Fourier transform as follows

$$u(\omega) = (2\pi)^{-1/2} \int_{-T_e/2}^{T_e/2} d\tau e^{-i\omega\tau} u(\tau) \quad (6)$$

where the function  $u(\tau)$  is defined on the interval  $-T_e/2 < \tau < T_e/2$  with periodic boundary conditions. Then using the theorem of residues

$$u(\omega) = i(2\pi)^{1/2} \sum_j R_j \exp(i\omega x_j - |\omega y_j|) \quad (7)$$

where  $R_j$  are the poles residue and  $x_j + iy_j$  are their location in the relevant half plane of the complex time, one obtains asymptotic behavior of the spectrum  $E(\omega) = |u(\omega)|^2$  at large  $\omega$

$$E(f) \sim \exp(-4\pi f y_{min}) \quad (8)$$

where  $\omega = 2\pi f$  and  $y_{min}$  is the imaginary part of the location of the pole which lies nearest to the real axis.

If in the considered case  $y_{min} = 1d$ , then we obtain the exponential decay shown in Fig. 1 (cf Eq. (1)). In order to understand the reason for  $y_{min} = 1d$  we need in a nonlinear dynamic climate model where the *daily* periodic solar impact results in such position of the pole nearest to the real axis. But even before constructing such dynamic model it is already clear that just the *daily* periodicity of the solar impact is responsible for the chaotic exponential decay shown in Fig. 1.

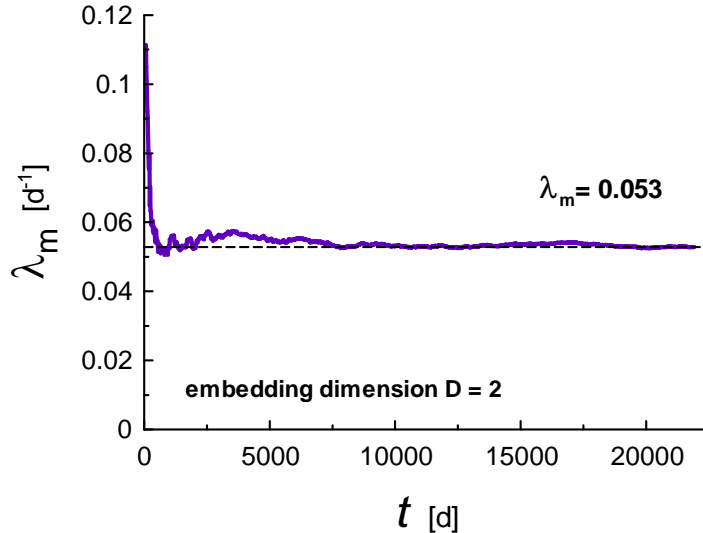


Figure 5: The pertaining average maximal Lyapunov exponent at the pertaining time, calculated for the same data as those used for calculation of the spectrum (Fig. 1). The dashed straight line indicates convergence to a positive value.

A confusion can arise due to the 1 day period also being the sampling frequency for the NAO and SOI time series. However, the poles location in the complex time plane is presumably determined by the system's *dynamics* and not by the sampling rate. For the considered above examples, for instance, the exponential decay rate (Figs. 3 and 4) is not equal to  $4\pi s$ ,  $s$  being the sampling rate for the corresponding time series, as it would be otherwise.

Additionally to the exponential spectrum, let us check the chaotic character of the wavelet regression detrended NAO data set calculating the largest Lyapunov exponent :  $\lambda_{max}$ . A strong indicator for the presence of chaos in the examined time series is condition  $\lambda_{max} > 0$ . If this is the case, then we have so-called exponential instability. Namely, two arbitrary close trajectories of the system will diverge apart exponentially, that is the hallmark of chaos. To calculate  $\lambda_{max}$  we used a direct algorithm developed by Wolf et al. (1985), Kodba et al. (2003). Figure 4 shows the pertaining average maximal Lyapunov exponent at the pertaining time, calculated for the same data as those used for calculation of the spectrum (Fig. 1). The largest Lyapunov exponent converges very well to a positive value  $\lambda_{max} \simeq 0.053d^{-1} > 0$ .

#### 4. Conclusions

The exponential decay of the broad-band spectrum of the wavelet regression detrended NAO and SOI time series (Figs. 1 and 2) indicates a chaotic nature of the high-frequency components of these climate oscillations. In Fig. 1 one can readily recognize a peak corresponding to a dominant frequency of internal variability (corresponding to a period approximately equal to 40 days, cf. with the fundamental frequency of the chaotic systems: Figs. 3 and 4). It should be noted, that the 40-day oscillations are well known as an intrinsic mode of the Northern Hemisphere extratropics, which is excited presumably due to instabilities related to large-scale topography (see, for instance, Magana 1993; Marcus, Ghil and Dickey 1994; Ghil and Robertson 2002). In this case the dominant frequency of internal variability (corresponding to the period  $\sim 40$ d) is considerably smaller than the daily solar forcing frequency, which determines the rate of the spectral exponential decay (Eq. (8)). Thus, the exponential chaotic decay (Fig. 1) can be considered as a dissipation mechanism for these oscillations. Figure 2 shows analogous picture for the SOI data.

#### 5. Acknowledgments

I thank to J. Hurrell and to the Department of Environment and Resource Management (Queensland) for sharing their data.

## References

- Farmer J.D, 1982, Chaotic attractors of an infinite dimensional dynamic system, *Physica D*, **4**, 366-393.
- Frisch U. and R. Morf, 1981, Intermittency in non-linear dynamics and singularities at complex times, *Phys. Rev.*, **23**, 2673-2705.
- Ghil M., and A.W. Robertson, 2002, "Waves" vs. "particles" in the atmosphere's phase space: A pathway to long-range forecasting? *Proc. Natl. Acad. Sci.*, **99** (Suppl. 1), 2493-2500.
- Hurrell J.W. et al., 2003, An Overview of the North Atlantic Oscillation, in "The North Atlantic Oscillation: Climatic Significance and Environmental Impact", *Geophysical Monograph* **134**, p.1, American Geophysical Union (2003).
- Kodba S., Perc M., and Marhl M., 2005, Detecting chaos from a time series, *Eur. J. Phys.* **26**, 205-215.
- Magana V., 1993, The 40-day and 50-day oscillations in atmospheric angular momentum at various latitudes, *J. Geophys. Res.*, **98**, 10441-10450.
- Marcus S.L., Ghil M., and J.O. Dickey, 1994, The extratropical 40-day oscillation in the UCLA General Circulation Model, Part I: Atmospheric angular momentum, *J. Atmos. Sci.*, **51**, 1431-1466.
- Miles J. 1984, Chaotic motion of a weakly nonlinear, modulated oscillator, *PNAS*, **81**, 3919-3923.
- NAO, 2010a, <http://www.cgd.ucar.edu/cas/jhurrell/indices.html>
- NAO, 2010b, [http://www.cpc.ncep.noaa.gov/products/precip/CWlink/pna/nao\\_loading.html](http://www.cpc.ncep.noaa.gov/products/precip/CWlink/pna/nao_loading.html)
- Ogden T., 1997, *Essential Wavelets for Statistical Applications and Data Analysis*, Birkhauser, Basel.
- Ohtomo N. et al., 1995, Exponential Characteristics of Power Spectral Densities Caused by Chaotic Phenomena, *J. Phys. Soc. Jpn.*, **64**, 1104-1113.
- Ott E., 2002. *Chaos in Dynamical Systems* (Cambridge University Press).
- Permann D. and I. Hamilton, 1992. Wavelet analysis of time series for the Duffing oscillator: The detection of order within chaos, *Phys. Rev. Lett.*, **69**, 2607-2610.
- Sigeti D.E., 1995, Survival of deterministic dynamics in the presence of noise and the exponential decay of power spectrum at high frequencies. *Phys. Rev. E*, **52**, 2443-2457.
- SOI, 2010, <http://www.longpaddock.qld.gov.au/SeasonalClimate>

[Outlook/SouthernOscillationIndex/SOIDataFiles/index.html](#)

Troup A.J., 1965, The Southern Oscillation. *Quart. J. Roy. Met. Soc.*, **91**, 490-506.

Wolf A. et al., 1985, Determining Lyapunov exponents from a time series, *Physica D*, **16**, 285-317.